Spatial deformation models for non-rigid image registration

Peter Rogelj, Stanislav Kovačič
University of Ljubljana, Faculty of Electrical Engineering
Tržaška 25, 1000 Ljubljana
e-mail: peter.rogelj@fe.uni-lj.si, stanek@fe.uni-lj.si

Abstract

Spatial deformation models are used to regularize image registration such that they prevent physically and anatomically unlikely transformations. It is often assumed that optimal models are obtained by modeling deformation properties of real tissues. However, this is not exactly true, because external forces, which drive the registration, in general differ from forces which in reality deformed the anatomy. In order to develop better spatial deformation models, it is necessary to consider these differences. In this work we focus on convolution based models. We analyze advantages and disadvantages of two most commonly used spatial deformation models, i.e. elastic model, and incremental model, and two widely used convolution kernels: an elastic kernel and a Gaussian kernel. The result of this work is a new combined elastic-incremental model, suitable for non-rigid registration of medical images.

1 Introduction

Deformation of materials is in physics described by various physical laws. The same deformation properties characterizing real materials are usually expected from spatial deformation models that are used for non-rigid registration. However, in order to exactly model the behavior of realistic materials multiple physical laws must be employed. In practice, spatial deformation models follow only a single, the most characteristic physical law, i.e. elasticity [1, 4, 11, 12] or viscosity [3, 5, 6], and furthermore, this characteristic behavior is usually linearized. Thus, the deformation properties of real materials are usually approximated by linear models, which can still describe deformation properties of tissues sufficiently well, although their computational cost is considerably lower. Such spatial deformation models can be implemented using a couple of approaches. Initially, they were modeled exclusively by implementing corresponding partial differential equations [1], while later a finite element approach [9] and a convolution approach [3] were proposed. In this work we follow the convolution approach, proposed by Bro-Nielsen [2, 3]. The idea of this approach is that every linear model can be implemented by convolution filtering, where the filter kernel equals the impulse response of the deformable media. Such regularization can be applied to voxel displacements or to voxel velocities. Thus,

common spatial deformation models differ only in two aspects: according to the filter kernel and according to the data that is being filtered.

2 Convolution models

The most dominant deformation property of tissues is elasticity, which is in the case of convolution models implemented by filtering the total external forces, which cause the deformation [2]:

$$\mathbf{T} = \mathbf{G} * \mathbf{F}, \tag{1}$$

Here, $\mathbf{F}$ denote external forces, $\mathbf{G}$ is a convolution kernel, and $\mathbf{T}$ stands for the transformation that defines displacements of image voxels. However, in the case of image registration the total forces are not available, as external forces are only an estimate how the forces should act to *improve* similarity between the images. The equation (1) therefore cannot be used directly.

In order to solve this problem we separate the spatial deformation model into two parts. The first part follows the Hooke's law to compute unregularized displacement of image points, while the second part regularizes them according to the impulse response of the deformable media to obtain the final transformation $\mathbf{T}$, see Fig. 1. In accordance with this we separate the convolution filter $\mathbf{G}$ into two terms, a filter gain k_F and a normalized kernel $\mathbf{G}_E$, such that

$$\mathbf{G} = k_F \mathbf{G}_E, \tag{2}$$

$$\int \mathbf{G}_E(\mathbf{x}) d\mathbf{x} = \sum_{\mathbf{x}} \mathbf{G}_E(\mathbf{x}) = 1. \tag{3}$$

Elastic regularization can now be performed by filtering voxel displacements instead of external forces. In contrast to total external forces total voxel displacements are known in each registration iteration, which enables elastic as well as other types of spatial deformation models.

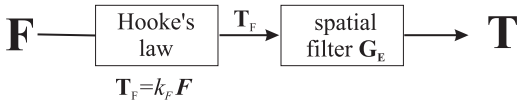

Figure 1: Convolution models can be separated into the Hooke's law, which maps external forces into a transformation (displacements) of independent image points, and spatial regularization filter $\mathbf{G}_E$, which models interdependencies between the points to regularize the transformation.

2.1 Elastic model

The characteristic of elastic materials is to deform due to applied external forces and return back into the undeformed configuration when the forces are retracted. This behavior requires regularization of total voxel displacements.

External forces obtained during the registration procedure tend to improve the transformation iteratively. Consequently, the transformation in the t-th iteration $\mathbf{T}^{(t)}$ is a sum of the transformation obtained in the previous iteration $\mathbf{T}^{(t-1)}$ and an increment $\mathbf{T}_F^{(t)}$ that follows the Hooke's law, and furthermore, all together must be regularized by the spatial regularization filter, see the block scheme in Figure 2:

$$\mathbf{T}^{(t)} = (\mathbf{T}^{(t-1)} + \mathbf{T}_F^{(t)}) * \mathbf{G}_E \tag{4}$$

This can be rewritten in the following form:

$$\mathbf{T}^{(t)} = \mathbf{T}_F^{(t)} * \mathbf{G}_E + \mathbf{T}_F^{(t-1)} * \mathbf{G}_E^2 + \mathbf{T}_F^{(t-2)} * \mathbf{G}_E^3 + ... + \mathbf{T}_F^{(1)} * \mathbf{G}_E^t, \tag{5}$$

where $\mathbf{G}_E^n$ stands for n-times convolution with filter $\mathbf{G}_E$. By increasing the number of convolution steps n the convolution kernel becomes wider and approaches towards averaging. Consequently, if the external forces do not exist ($\mathbf{F} = 0$), the model gradually returns back to the undeformed configuration. As forces in earlier iterations are regularized with wider kernels they contribute to more global matching, while forces in later iterations are regularized with narrower kernels and deal with more localized image mismatches. This is advantageous because the estimated forces do not act directly in the direction of the correct match, and thus include a local error. This is more obvious in initial registration iterations, when images are more mismatched, than in later registration iterations, when points used for estimating external forces are already close to their correct position.

The elastic models have also one important disadvantage. The problem appears because external forces exist only if there is some image mismatch, while they are necessary to maintain the deformed state of the image. Thus, local image discrepancies can never be registered absolutely correct as there is always some mismatch required to maintain the deformation. The mismatch is actually a systematic error and is larger for larger deformations. This makes the elastic model less suitable for large deformations, such that it is often replaced by viscous fluid or incremental models.

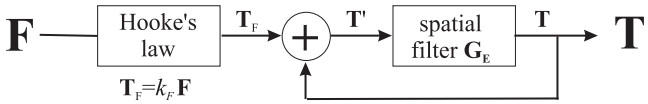

Figure 2: A block scheme of the elastic model suitable for iterative non-rigid registration procedures.

2.2 Incremental model

Incremental models were introduced to avoid systematic error of the elastic approach. They are based on the elasticity and assume that the total force $\mathbf{F}_0$, which is required for registering two images, can be obtained by summing the estimated external forces over all registration iterations:

$$\mathbf{F}_0 = \sum_t \mathbf{F}^{(t)}, \tag{6}$$

where t denotes the iteration number. Following the principle of linearity, the final transformation $\mathbf{T}$ can also be computed as a sum of partial transformations (displacements) $\mathbf{T}^{(t)}$

$$\mathbf{T} = k_F \mathbf{G}_E \sum_t \mathbf{F}^{(t)} = \sum_t \mathbf{G}_E \mathbf{T}_F^{(t)}, \tag{7}$$

and consequently,

$$\mathbf{T}^{(t)} = \mathbf{T}^{(t-1)} + \mathbf{G}_E \mathbf{T}_F^{(t)}, \tag{8}$$

A block scheme of incremental spatial deformation model is shown in Fig. 3. The incremental model considerably differs from the deformation properties of real tissues. When forces are retracted the material remains in the deformed configuration. Incremental model also enables very large deformations, even such that are not expected for real tissues. The disadvantage of this approach is in accumulation of registration error. External forces do not always act exactly in the direction of the correct match, especially not in initial registration steps, and this differences represent an error. The error accumulates in point displacements and cannot be corrected in later registration iterations, such that it also reflects in the registration error. Thus, the ability to perform large image deformation is related to reduced anatomical suitability, which reflects in larger registration error. This is the main disadvantage of the incremental model.

Figure 3: A block scheme of the incremental model.

2.3 Combined elastic-incremental model

Elastic as well as incremental models have certain advantages and certain disadvantages. The elastic model provides physically and anatomically reasonable deformation properties and thus assures relatively low registration error for information poor image regions, e.g. homogeneous image regions. However, it suffers from the systematic error, which is the most obvious in information rich regions, e.g. edges of anatomical structures may not perfectly overlap. On the other hand, deformation properties of the incremental model and the viscous model differ from deformation properties that are expected for most real tissues, which results in higher registration errors in information poor image regions. However, because these models do not suffer from the systematic error, they better register information rich image regions.

In order to improve the registration we have devised a combined elastic-incremental model, which combines advantages of elastic and incremental models. The elastic part is expected to contribute to low registration error for information poor image regions, while the incremental part is expected to aid to matching of information rich image regions. The obtained model consists of two convolution filters, where the first one, $\mathbf{G}_I$, follows the principle of the incremental model and regularizes transformation improvements $\mathbf{T}_F$, and the second filter, $\mathbf{G}_E$,

represents the elastic properties and regularizes the overall transformation $\mathbf{T}$, see the block scheme in Figure 4:

$$\mathbf{T}^{(t)} = (\mathbf{T}^{(t-1)} + \mathbf{T}_F^{(t)} * \mathbf{G}_I) * \mathbf{G}_E \tag{9}$$

The first filter ($\mathbf{G}_I$) enables large deformations and precise registration while the second one ($\mathbf{G}_E$) serves to improve the linearity of the results. The total regularization $\mathbf{G}$, i.e. the normalized impulse response of the combined model, suits to the convolution of both filter kernels:

$$\mathbf{G} = \mathbf{G}_I * \mathbf{G}_E. \tag{10}$$

If Gaussian filters are used then the obtained total standard deviation is

$$\sigma_{\mathbf{G}} = \sqrt{\sigma_{\mathbf{G}_I} + \sigma_{\mathbf{G}_E}}. \tag{11}$$

The behavior of the combined spatial deformation model depends on the ratio between regularization provided by each of the filters, such that in the extreme cases the incremental model is obtained when $\mathbf{G}_E = \delta$ and the elastic model is obtained when $\mathbf{G}_I = \delta$. Here δ is a Dirac's delta function. If both filters differ from δ, then the improvements are expected.

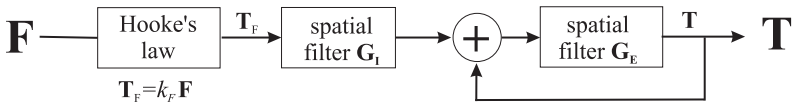

Figure 4: A block scheme of the combined elastic-incremental model.

3 Filter kernels

Kernels of the convolution filters define spatial deformation properties of the modeled material. Firstly, the kernel width defines stiffness of the model, such that wider kernels correspond to more stiff materials and narrower kernels correspond to more flexible materials. Secondly, the type of the kernel defines some other characteristics of the deformation, e.g. compressibility, isotropy, etc. In order to realistically model elasticity and viscosity Bro-Nielsen and Gramkow proposed an elastic kernel [2, 3, 10], see Figure 5 left. The alternative is a Gaussian kernel, see Figure 5 right, which can be regarded as a separable approximation to the elastic kernel. Due to the separability it additionally reduces the computational cost and substantially increases registration speed, which is the main reason why Gaussian kernels have been extensively used. A disadvantage of separable kernels is that due to independence of spatial dimensions they do not provide control over compressibility, such that longitudinal stretch does not induce a lateral shrink.

Although it is often assumed that realistic kernels enable better registration, this not necessarily true. The reason for this is in external forces that drive the registration, which should, in order to perfectly recover the deformation, equal the forces that deformed the anatomy. This is never the case, because images do not provide enough information to enable assessment

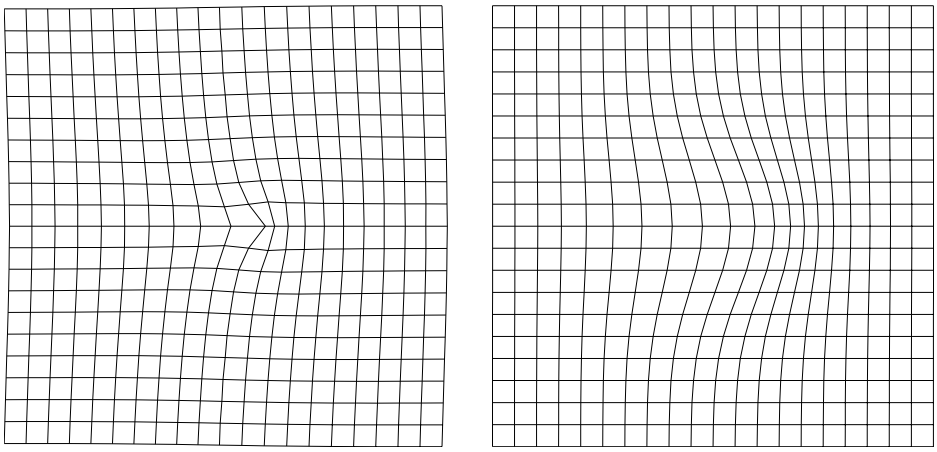

Figure 5: An example of elastic kernel (left) and Gaussian kernel (right) presented by a deformed grid.

of transformation in homogeneous image regions. Consequently, external forces act only on information rich image regions, i.e. edges of imaged anatomical structures.

If forces that deform the anatomy actually act only on the edges of anatomical structures, then realistic kernels do enable good registration. A one dimensional illustration of such case is shown in Figure 6. The deformation caused by force $\mathbf{F}_0$ can be perfectly recovered when using kernel that equals the impulse response of deformed media, because external forces $\mathbf{F}_R$ can be estimated correctly. Gaussian kernels in this case cause larger registration error. The point on the edge is still correctly transformed, see $\mathbf{T}(x_{F_0})$, such that images still look equal, but transformation deviates from the ideal one in points inside homogeneous image regions ($x \neq x_{F_0}$).

The situation is different if forces $\mathbf{F}_0$ that deform the anatomy act on homogeneous image regions and not on edges of anatomical structures, see Figure 7. In this case external forces $\mathbf{F}_R$ cannot be estimated correctly and still act only on edges of anatomical structures. Although points on the edges can still be registered correctly and images may look equal after the registration, transformation inside homogeneous image regions cannot be assessed correctly. Our example in Figure 7 shows that in such cases registration can be more correct if less realistic kernels, e.g. Gaussian, are used instead of realistic ones, e.g. elastic kernels.

The experiments show that the best registration results are not necessarily obtained by spatial deformation models that exactly follow deformable properties of the anatomy. This justifies the use of Gaussian models, which are often used due to their lower computational cost. The selection and setting of the model is therefore not straightforward an depends on the application, specifically on the expected distribution of body forces, required compressibility and volume preservation, etc. Because of all this we use Gaussian kernels and not elastic ones.

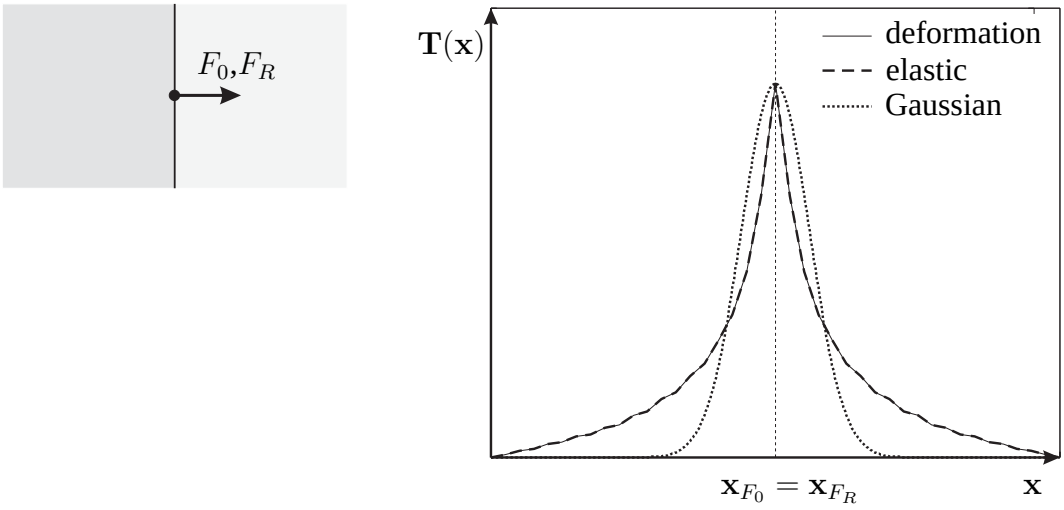

Figure 6: If a force F_0 that deform the anatomy acts on the edge of some imaged structure as illustrated on the left hand side, the medium deforms as shown on the graph by thin solid line. The estimated external force F_R acts on the same image point (see illustration on the left) such that images can be correctly registered using kernel that equals the impulse response of the medium (see the graph, dashed line). If Gaussian kernel is used the deformation cannot be perfectly recovered and some registration error exists (dotted line).

4 Results

We have compared the combined elastic-incremental model with the elastic and the incremental model. Comparison was based on recovering synthetic deformations. The synthetic deformation was generated as a sum of six three-dimensional Gaussian functions with standard deviation ranging between 15 and 60 mm, such that the initial RMS displacement error was $e_{RMS} = 7.09$ mm and the maximal displacement error was $e_{max} = 16.84$ mm. The experiment was performed using two spatially aligned Brainweb [7, 8, 13] images of human head with voxel size $1 \times 1 \times 1$ mm. The first image, MRI-PD, was synthetically deformed and used as the target for registering the other image, MRI-T1. Gaussian convolution kernels were used for the regularization, such that the standard deviation of the overall regularization was in all the cases the same, $\sigma_{\mathbf{G}} = 4.24$. The comparison was made between the results for nine different settings of the combined spatial deformation model, where one of the settings suited to the elastic model ($\sigma_{\mathbf{G}_I} = 0$,$\sigma_{\mathbf{G}_E} = 4.24$) and one to the incremental model ($\sigma_{\mathbf{G}_I} = 4.24$,$\sigma_{\mathbf{G}_E} = 0$). In all the cases the coefficient k_F was recomputed in each iteration, such that the increment $\mathbf{T}_F(\mathbf{x})$ was limited to the size of one image voxel. The comparison was made for three resolution levels of a multiresolution registration strategy. First, images subsampled by factor 4 were registered in resolution level 2, then the registration continued in level 1 with images subsampled by factor 2, and finally, the original images were registered in level 0. The best result of each level (with respect to maximal displacement error e_{max}) was used as the initial deformation for the next resolution level. The results are tabulated in Table 1.

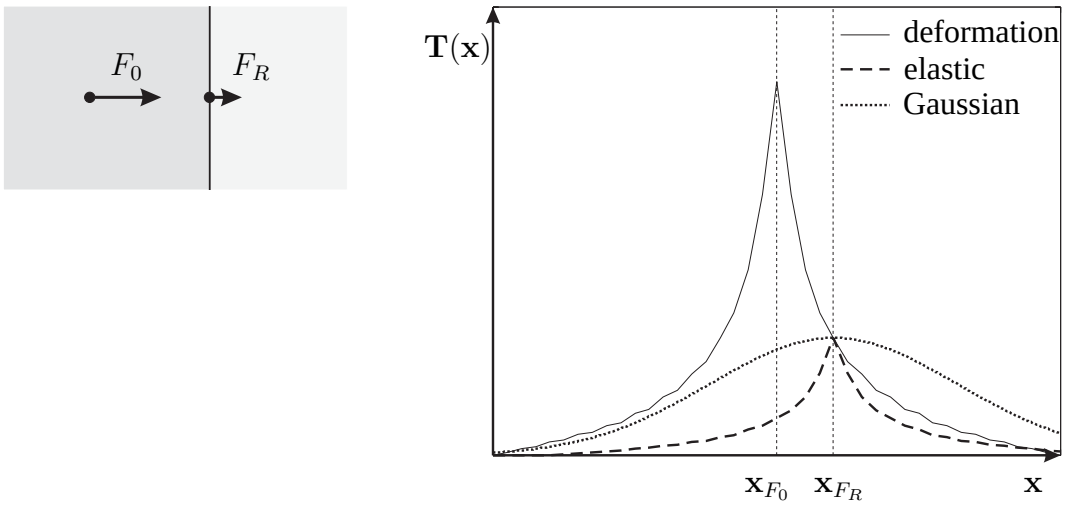

Figure 7: If a force F_0 that deform the anatomy acts on a point inside a homogeneous image region as illustrated on the left hand side, the medium deforms as shown on the graph by thin solid line). The estimated external force F_R does not act on the same image point, but on the edges of anatomical structures (see illustration on the left). Images cannot be correctly registered, not even by using realistic kernels (see the graph, dashed line). In such cases some less realistic kernels, e.g. Gaussian (dotted line), may cause lower registration error. In the presented experiment the Gaussian kernel (dotted line) is more suitable than the elastic kernel (dashed line) and yields a 30% lower RMS registration error.

In all three resolution levels the best results were obtained when both of the filters of the combined model were employed. Thus, the combined model performed better than the incremental or the elastic model. The elastic model resulted in a large registration error due to small external forces, which were limited in order to limit the change of transformation in one registration iteration to the size of one image voxel. Consequently, the registration cannot result in deformations larger than those, that can be maintained by such small external forces. On the other hand, the incremental model also results in larger errors than the optimal combined model, which is due to non-linear relationship between external forces and required image transformation. The best results were obtained when both of the convolution filters were used, such that elastic and incremental properties were combined. In general an optimal ratio between elastic and incremental regularization may depend on the type of deformations that are being recovered.

5 Conclusion

In this paper we focused on spatial deformation models based on convolution. We proposed a new combined elastic-incremental model and compared it with the elastic model and the incremental model. The combined model tends to reduce the systematic error of the elastic

Table 1: Evaluation results for the combined elastic-incremental spatial deformation model

		Level 2			Level 1			Level 0		
$\sigma_{\mathbf{G}_I}$	$\sigma_{\mathbf{G}_E}$	e_{RMS}	e_{max}	CC	e_{RMS}	e_{max}	CC	e_{RMS}	e_{max}	CC
0.00	4.24	5.03	14.05	0.9206	3.19	11.32	0.9626	1.51	6.19	0.9827
0.50	4.21	4.72	13.60	0.9305	2.96	10.93	0.9671	1.39	5.95	0.9840
1.00	4.12	4.11	12.85	0.9444	2.44	9.98	0.9751	1.16	5.33	0.9856
2.00	3.74	3.16	11.42	0.9565	1.44	7.25	0.9819	0.76	3.82	0.9869
3.00	3.00	2.13	8.40	0.9657	0.80	3.74	0.9838	0.50	2.62	0.9870
3.74	2.00	1.37	4.68	0.9523	**0.55**	1.95	0.9837	**0.39**	1.97	0.9863
4.12	1.00	1.30	4.13	0.9532	0.59	2.41	0.9827	0.43	1.78	0.9857
4.21	0.50	**1.17**	4.64	0.9611	0.68	2.83	0.9806	0.49	1.80	0.9854
4.24	0.00	1.49	4.95	0.9523	0.73	3.09	0.9809	0.51	1.92	0.9852

model and the accumulated error of external forces, which is characteristic for the incremental model. It turns out that these two errors are related, such that the decrease of the first one increases the second one, and vice versa. The combined model enables to find an optimum, where the total error is the lowest. The comparison results prove that the combined model does perform better than the other two models individually. However, the optimal settings, including the ratio between elastic and incremental regularization, may depend on the nature of the deformation.

Wa have also analyzed and compared two different convolution kernels: the elastic kernel and the Gaussian kernel. The elastic kernel models the real tissue properties better than the Gaussian kernel. Its major advantage is to provide control over the material compressibility and thus enable volume preservation. As expected it turned out that it gives better results when the anatomy is deformed by forces that act on the edges of anatomical structures. If this is not the case, the situation is more difficult and transformation cannot be recovered exactly. It turns out that in the case, when forces act in homogeneous image regions, the realistic elastic model gives even worse results than some other, nonrealistic models, because estimated external forces differ from the ones that actually deformed the tissues. This justifies the use of Gaussian models, which have an additional advantage of lower computational cost.

References

[1] R. Bajcsy and S. Kovačič. Multiresolution elastic matching. *Computer Vision, Graphics and Image Processing*, 46:1–21, April 1989.

[2] M. Bro-Nielsen. *Medical Image Registration and Surgery Simulation*. PhD thesis, Department of Mathematical Modelling, Technical University of Denmark, 1996.

[3] M. Bro-Nielsen and C. Gramkow. Fast fluid registration of medical images. *Springer Lecture Notes in Computer Science*, 1131:267–276, 1996.

[4] G.E. Christensen and H.J. Johnson. Consistent image registration. *IEEE Transactions on Medical Imaging*, 20(7):568–582, July 2001.

[5] G.E. Christensen, R.D. Rabbit, and M.I. Miller. A deformable neuroanatomy textbook based on viscous fluid mechanics. In Prince and Runolfsson, editors, *Proceedings of the 1993 Conference on Information Sciences and Systems*, pages 211–216. Johns Hopkins University, 1993.

[6] G.E. Christensen, R.D. Rabbitt, and M.I. Miller. Deformable templates using large deformation kinematics. *IEEE Transactions on Image Processing*, 5(10):1435–1447, 1996.

[7] C. A. Cocosco, V. Kollokian, R.K.-S. Kwan, and A.C. Evans. Brainweb: Online interface to a 3D MRI simulated brain database. In *NeuroImage*, volume 5, May 1997.

[8] D.L. Collins, A.P. Zijdenbos, V. Kollokian, J.G. Sled, N.J. Kabani, C.J. Holmes, and A.C. Evans. Design and construction of a realistic digital brain phantom. In *IEEE Transactions on Medical Imaging*, volume 17, pages 463–468, June 1998.

[9] J. C. Gee, D. R. Haynor, M. Reivich, and R. Bajcsy. Finite element approach to warping of brain images. In M. H. Loew, editor, *Proc. SPIE Medical Imaging 1994: Image Processing*, volume 2167. SPIE Press, Bellingham, WA, 1994.

[10] C. Gramkow and M. Bro-Nielsen. Comparison of three filters in the solution of the navier-stokes equation in registration. In *Proceedings of the Scandinavian Conference on Image Analysis – SCIA'97*, pages 795–802, 1997.

[11] A. Hagemann, K. Rohr, H.S. Stiehl, U. Spetzger, and J.M. Gilsbach. Biomechanical modeling of the human head for physically based, nonrigid image registration. *IEEE Transactions on Medical Imaging - Special Issue on Model-Based Analysis of Medical Images*, 18(10):875–884, 1999.

[12] N. Hata, T. Dohi, S.K. Warfield, W.M. Wells, R. Kikinis, and F.A. Jolesz. Multimodality deformable registration of pre- and intraoperative images for MRI-guided brain surgery. In W.M. Wells, A. Colchester, and S. Delp, editors, *Proceedings of the 1st International Conference on Medical Image Computing and Computer-Assisted Intervention – MICCAI'98*, number 1496 in Lecture Notes in Computer Science, pages 1067–1074, MIT, Cambridge, MA, USA, October 1998. Springer-Verlag.

[13] R.K.-S. Kwan, A.C. Evans, and G. B. Pike. An extensible MRI simulator for post-processing evaluation. In *Visualization in Biomedical Computing (VBC'96)*, volume 1131 of *Lecture Notes in Computer Science*, pages 135–140. Springer-Verlag, May 1996.